Enhanced photocatalytic activity of octahedral anatase particles prepared by hydrothermal reaction

Z. Wei[a], E. Kowalska[a,*], K. Wang[a], C. Colbeau-Justin[b], B. Ohtani[a]

[a] Institute for Catalysis, Hokkaido University, N21, W10, 001-0021 Sapporo, Japan

[b] Laboratoire de Chimie Physique, CNRS UMR 8000, Université Paris-Saclay, Bat. 349, 91405 Orsay, France

* Corresponding author. Tel.: +81 117069130,

E-mail address: kowalska@cat.hokudai.ac.jp (E. Kowalska);

ABSTRACT

Octahedral anatase particles (OAPs) were prepared by hydrothermal reaction (HT) with various experimental conditions, including different amounts of titanate nanowires (TNWs), different water volumes and different pH values, to obtain products with high contents of OAPs. The properties of photocatalysts were investigated by XRD, SEM, TEM, XPS and time-resolved microwave conductivity (TRMC). Photocatalytic activities for oxidative decomposition of acetic acid (CO_2 system) and anaerobic dehydrogenation of methanol (H_2 system) were tested. It was found that a larger amount and concentration of TNWs, as well as higher pressure during HT, resulted in the formation of smaller crystallites with higher density of mobile electrons. Enhanced photocatalytic activity, achieved for samples with the best morphology (higher content of OAPs), correlated with slower TRMC signal decay, i.e., slower recombination of charge carriers (e^-/h^+) probably due to lower content of deep electron traps. It was found that properties of platinum nanoparticles, deposited in-situ in the H_2 system in the absence or presence of pre-sparged oxygen, and their connection with OAPs were decisive factors for photocatalytic activity.

Keywords: anatase; morphology; OAPs; octahedral particles; photocatalytic activity; platinum nanoparticles

1. Introduction

Titanium(IV) oxide (titania, TiO_2) has been widely applied for environmental purification because of its many advantages such as good stability, strong redox ability, nontoxicity, cheapness and high availability [1, 2]. The influence of titania structural/physical properties on the photocatalytic activity has been extensively studied. Results of previous studies suggested that higher crystallinity, larger specific surface area, smaller crystalline size and specific morphology (exposed crystal facets) resulted in higher photocatalytic activity [3, 4].

Although particle morphology has been suggested to be an important factor for the activity of the photocatalyst [3, 5-8], no direct proof was presented for that until our recent study in which the morphology of octahedral anatase particles (OAPs) was shown to be a key factor for the photocatalytic activity [9]. Direct evidence for OAP

samples possessing almost the same properties (crystallinity, crystalline size, specific surface area and total amount of electron traps) and differing only by morphology has been presented, i.e., direct correlation between morphology and photocatalytic activity. It has been proposed that facetted anatase of an octahedral shape is responsible for the preferential distribution of shallow electron traps (ETs) rather than deep ETs, enabling greater mobility of electrons instead of their permanent trapping.

Titania with different morphologies has been prepared by various methods including hydrothermal reaction (HT), solvothermal, sol-gel, elecrtosynthesis and gas-phase methods [8, 10-12]. HT is one of the most popular methods for titania synthesis due to feasible preparation of required nanostructures by simply changing the process conditions [3]. It is possible to modulate all HT conditions including HT temperature [6], HT duration [3, 6], precursor amount, additives content [13], solvent volume [14], pH value of the reaction suspension [3], and pre- and post-treatment operations such as ultrasonication, calcination and grinding. For example, it was reported that crystal phase, shape and size of titania particles depended significantly on pH value of the peroxo titanic acid solution and HT duration [3].

Our previous study showed the effects of HT temperature, HT duration, ultrasonication duration, calcination and grinding on preparation of OAPs [15, 16]. It was found that morphology governed photocatalytic activity, i.e., the higher the OAP content was in the final product, the higher was the photocatalytic activity. It is thought that changes in the content of reagents and pressure during the HT process (suspension/air ratio) influence the morphology of the final product and thus its photocatalytic activity. Therefore, in the present study, contents of the precursor and water as well as pH value of the reaction suspension were investigated.

2. Materials and methods

Potassium titanate nanowires (TNWs), prepared by HT of Evonik P25 titania (Nippon Aerosil) and potassium hydroxide solution [17], were used as the precursor for fabrication of titania samples containing OAPs. TNWs (100 - 1067 mg) were ultrasonically dispersed in Milli-Q water (30-40 mL) for 1 h, and then the suspension was put into a 100-mL sealed Teflon bottle into which an additional portion of Milli-Q water (20 or 40 mL) was added when necessary. The bottle was placed into an outer sleeve of a stainless autoclave and then heated in an oven for 6 h at 433 K. The obtained suspension was dispersed by ultrasonication for 10 minutes and then centrifugally separated (12000 rpm, 20 minutes). The white precipitates were collected and dried overnight under vacuum (353 K, 12 h). HT processes were performed for seven weights of TNWs (100, 133, 200, 267, 400, 533 and 1067 mg) and three volumes of water (30, 60 and 80 mL). The codes of the samples were defined as follows: TNW amount/water volume. For example, a 267/80 sample was prepared with 267 mg of TNWs and 80 mL of water.

The morphology was characterized by electron microscopy (SEM, TEM and STEM). Crystalline size and aspect ratio were estimated by XRD analysis Experimental details are presented in SI.

The oxidation states of elements and surface compositions of samples were

determined by X-ray photoelectron spectroscopy (XPS), and charge-carrier dynamics was determined by the time-resolved microwave conductivity (TRMC) method (details in SI).

Photocatalytic activities for (a) oxidative decomposition of acetic acid and (b) anaerobic dehydrogenation of methanol were examined. In each experiment, 50 mg of the photocatalyst was suspended in 5 mL of aqueous solution containing (a) 5.0-vol% acetic acid and (b) 50-vol% methanol and then photoirradiated under (a) air and (b) argon with magnetic stirring. Photoirradiation (>290 nm) was performed using a 400-W high-pressure mercury lamp under thermostatic control at 298 K. In the case of reaction (b), hexachloroplatinic acid was added before photoirradiation to be reduced in situ by photoexcited electrons to zero-charged platinum metallic deposits. Amounts of liberated CO_2 (a) and H_2 (b) in gas phase were determinated by gas chromatography (TCD-GC). The photocatalytic activities are presented as relative values to those of the commercial anatase titania photocatalyst FP-6 (Showa Denko Ceramics) that was simultaneously tested (details in SI).

To prepare smaller platinum NPs, Pt was also deposited for oxygen-saturated suspension (15-min pre-bubbling), in which photogenerated electrons were firstly consumed by oxygen hindering formation of platinum NPs (Fig. S2).

3. Results and discussion

3.1. Influence of the content of reagents

3.1.1. Photocatalyst characterization

The yield of the HT process was 60-76% with only the exception of the sample prepared with the smallest content of reagents (100/30), for which 48% yield was obtained. XRD patterns of HT products are presented in Fig. 1. Preparation conditions of HT were the same for all samples, i.e., 1-h ultrasonication, 433-K HT, 6-h HT, under which samples with the best morphology (highest content of OAPs) and thus highest photocatalytic activity could be obtained [9]. It was confirmed by XRD analysis that these conditions are sufficient for efficient conversion of TNWs into anatase. Crystallographic characteristics of all samples were almost the same, i.e., the same position and intensity of XRD peaks, indicating that the content of reagents did not influence crystallinity. Magnification of a representative XRD pattern (Fig. 1, center) showed that only one crystalline phase was formed during the HT process, i.e., anatase, being in agreement with the results of our previous study showing that samples prepared under the same HT conditions possessed almost the same crystallinity, while shortening of the HT and lowering of its temperature resulted in incomplete reaction and thus in the presence of TNWs in the final products [9]. Similarly, pre- and post- treatment operations such as ultrasonication, calcination (even up to 1173 K) and grinding did not influence the crystallinity of OAP-containing samples [16]. Therefore, it is concluded that only temperature and duration of the HT process are decisive for crystallinity of OAP-containing samples, while the effects of concentration and pressure during the HT process as well as pre- and post-treatment operations on anatase formation are negligible. The HRTEM image of the 267/80 sample confirmed the presence of single

crystalline anatase (Fig. 1, right) due to a 0.35-nm lattice distance between fringes and the angle of 68.3° between (001) and (101) facets corresponding to anatase crystals, as has already been reported [7]. Crystalline sizes changed only in a narrow range from 15.8 to 17.8 nm, confirming the independence of crystalline properties on content of reagents.

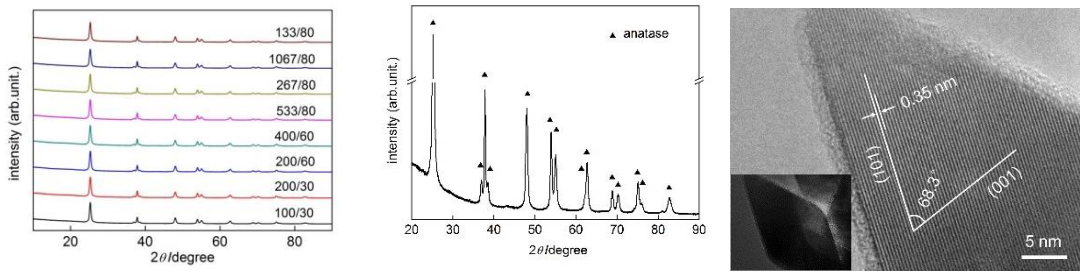

Fig. 1. (left) XRD patterns of all samples and (center) XRD pattern of the 267/80 sample with the corresponding TEM image (right).

Although, there was little variation in crystalline size, there was a clear correlation between the size and reagent content, especially for amount of TNWs, as shown in Fig. 2 (left). It was found that crystalline size decreased with increase in both the amount and concentration of TNWs (Fig. S3). However, a reverse correlation was found for aspect ratio (AR) change, i.e., increase of AR with increase in concentration of TNWs, suggesting that larger crystallites possessed smaller AR, as shown in Fig. 2 (right). These findings indicate that a higher concentration of TNWs results in either a steric effect and/or squeezing force, causing formation of elongated and smaller NPs. Obviously, this also results in simultaneous deformation of the perfect octahedral shape possessing an aspect ratio of 1.59. It is thought that additional four (100) facets can be formed between two (101) pyramids (nanoparticles encircled in Fig. 3), as was proposed for anatase nanorods prepared with hydrogen titanate in the presence of NaCl [14]. Summarized data are shown in Table S1.

The results of our previous study showed that changes in the conditions of HT (HT temperature, HT duration and US duration) resulted in a change in AR only in a narrow range of 1.6-1.8 [15]. On the other hand, post-treatment operations resulted in simultaneous changes in both crystalline size and AR in broad ranges of 17-110 nm and 0.7-1.7, respectively, i.e., temperature increase caused sintering and fusion of crystallites. For example, calcination at 1173 K resulted in formation of crystallites of 110 nm possessing AR of only 0.72. Present data indicate diminishing and narrowing of crystallites, resulting in the highest AR of ca. 1.9 for samples prepared with higher concentration of TNWs (6.66 g mL^{-1}) and larger volumes of water (60 and 80 mL). It is known that one of the most important parameters during the HT process is water volume, which directly correlates with remaining free space and thus with resultant pressure during the reaction. Moreover, change in solvent volume or precursor amount results in change in concentration. It should be pointed out that the 133/80 sample possessing an almost ideal AR of 1.61 was prepared with the largest volume but with the smallest amount and concentration of TNWs. Therefore, it is

concluded that concentration of TNWs rather than pressure inside the reactor is decisive for formation of perfect anatase crystals.

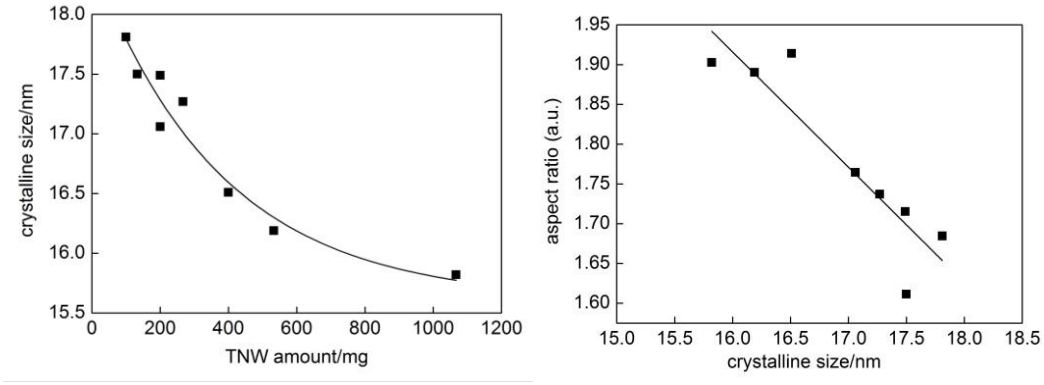

Fig. 2. (left) Influence of the amount of TNWs on crystalline size and (right) influence of crystalline size on AR.

The morphology of samples was investigated by SEM observation, and exemplary SEM images with respective values of total OAP content are shown in Fig. 3. It is clear that different morphologies were obtained for OAP products prepared under different synthesis conditions. The 267/80 and 533/80 samples had the highest and the lowest contents of OAPs, respectively. In general, an increase in the concentration of TNWs resulted in a decrease in OAP content. For example, an increase in the concentration from 3.33 to 6.66 g mL^{-1} caused decreases in OAP content from 50 to 45%, 53 to 48% and 64 to 41% for water volumes of 30, 60 and 80 mL, respectively. Therefore, results for morphology confirmed the crystallinity data, i.e., a higher concentration of TNWs induced deformation of the octahedral shape, i.e., increase in AR and decrease in crystalline size.

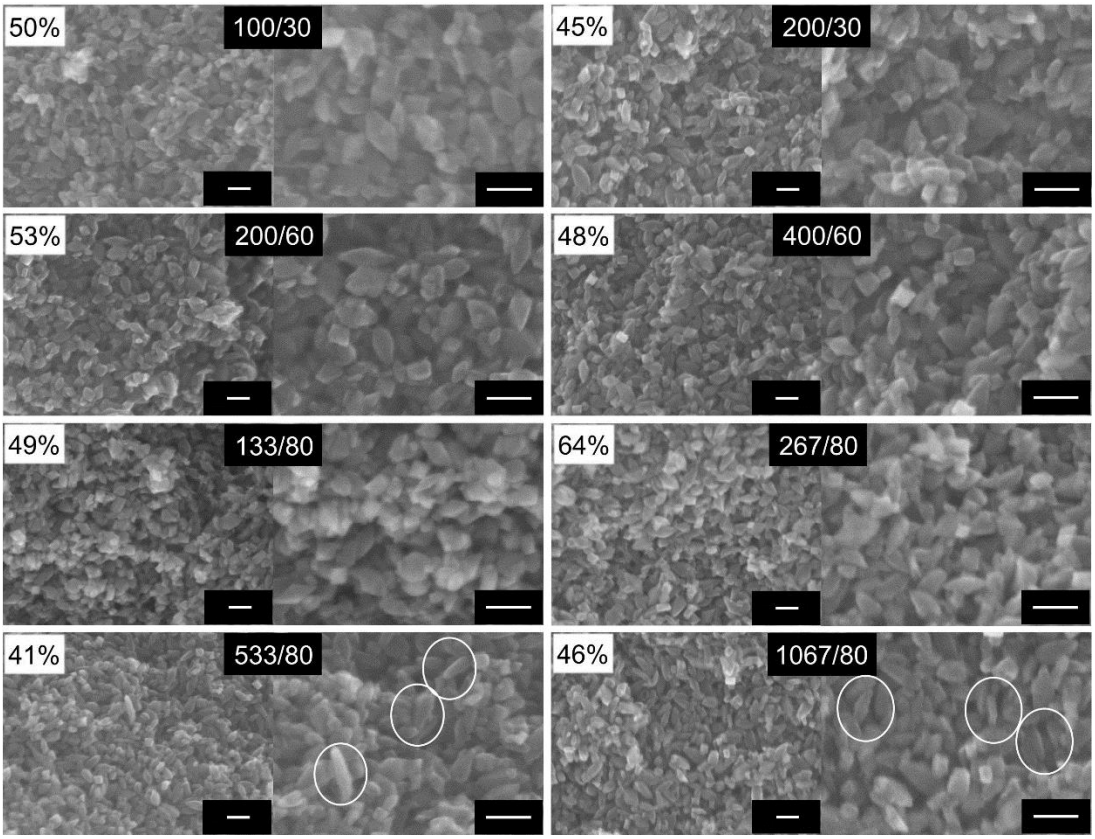

Fig. 3. SEM images of products prepared under different conditions with sample codes and total OAP content (in percent) shown in the images: Scale bars correspond to 50 nm and elongated particles are encircled.

Interestingly, the volume of water, and therefore pressure inside the reactor, seems to be crucial for preparation of perfectly shaped crystals but only at a low concentration of TNWs (3.33 g mL^{-1}). For example, an increase in the volume of water from 30 to 60 mL and then to 80 mL caused improvement of morphology, i.e., OAP contents of 50%, 53% and 64%, respectively. However, the correlation between morphology and concentration for the largest water volume (80 mL) was not clear, and it was concluded that optimal concentration resulted in improved morphology. These data are in contradistinction to AR, which was proportional to concentration of TNWs. It is proposed that SEM analysis is more precise for morphology characterization since particles are counted one by one, while mean values are obtained from XRD analysis.

To characterize surface composition of the samples, oxygen, titanium and carbon were analyzed by XPS method and the data obtained are discussed in detail in SI (Table S2 and Fig. S4). Briefly, the O:Ti ratio and form of oxygen significantly differed between the samples. For example, oxygen in the form of hydroxyl groups was predominant in the 267/80 sample, while it was mainly bounded (as TiO_2) in the 533/80 sample. It was found that the composition of samples was correlated with the form of oxygen in the samples, e.g., an increase in the amount of TNWs resulted in simultaneous increases in the content of hydroxyl groups and O:Ti ratio. Titanium was mainly present in the form of Ti^{+4} in all samples, and there was almost no difference in the form of carbon in the samples.

TRMC measurements were performed for evaluation of the mobility and lifetime of charge carriers, and the data obtained are shown in Fig. 4. Two parameters were determined in the analysis: i) maximum intensity of the TRMC signal (I_{max}) corresponding to overall mobility of photoexcited electrons in a relaxed state after laser excitation and ii) rate of signal decay. There are at least two reasons for the signal decay: decrease in the number (density) of electrons due to recombination with trapped holes and decrease in mobility due to trapping in deep electron traps (ETs). Since TRMC signal decay profiles could not be fitted with a single exponential function in general, the extents of decay were evaluated by decreases after 40 and 4000 ns as I_{40}/I_{max} and I_{4000}/I_{max}, respectively.

Enhancement of I_{max} was noticed with an increase in the value of every tested parameter, i.e., amount of TNWs, concentration of TNWs and volume of water, and linear dependence was obtained when at least one parameter was constant as shown in Figs. 4c and S5. It is thought that a larger amount and concentration of TNWs, as well as higher pressure during HT causing the formation of smaller crystallites (Fig. 2), result in products with higher density of mobile electrons (Fig. 4d). This is reasonable since a larger amount of ETs has already been reported for titania photocatalysts with smaller crystallite sizes [18]. Therefore, it is concluded that decrease in crystallite size results in the formation of products with a large amount of shallow ETs in which electrons can be easily detrapped.

However, in the case of signal decay, almost the same courses were obtained for samples prepared with smaller volumes of water (30 and 60 mL). For those samples, only the value of I_{max} varied i.e., I_{max} increased with increase in the amount of TNWs. On the other hand, for samples prepared with the largest volume of water, all decays differed significantly. The fastest decay of the 533/80 sample indicated that generated electrons were permanently trapped in deep ETs and/or were rapidly recombined with holes. The slowest decays were obtained for samples prepared with the largest volume of water and small content of the precursor (133/80 and 267/80), indicating that high pressure and low concentration during the HT process resulted in the formation of products with a favorable distribution of shallow ETs rather than deep ETs. To confirm this hypothesis, reverse photoacoustic spectroscopy, which enables determination of the distributions of shallow ETs and deep ETs, will be performed. It is expected that slow decay and high I_{max} of the 267/80 sample should result in enhanced photocatalytic activity, as discussed in the next section.

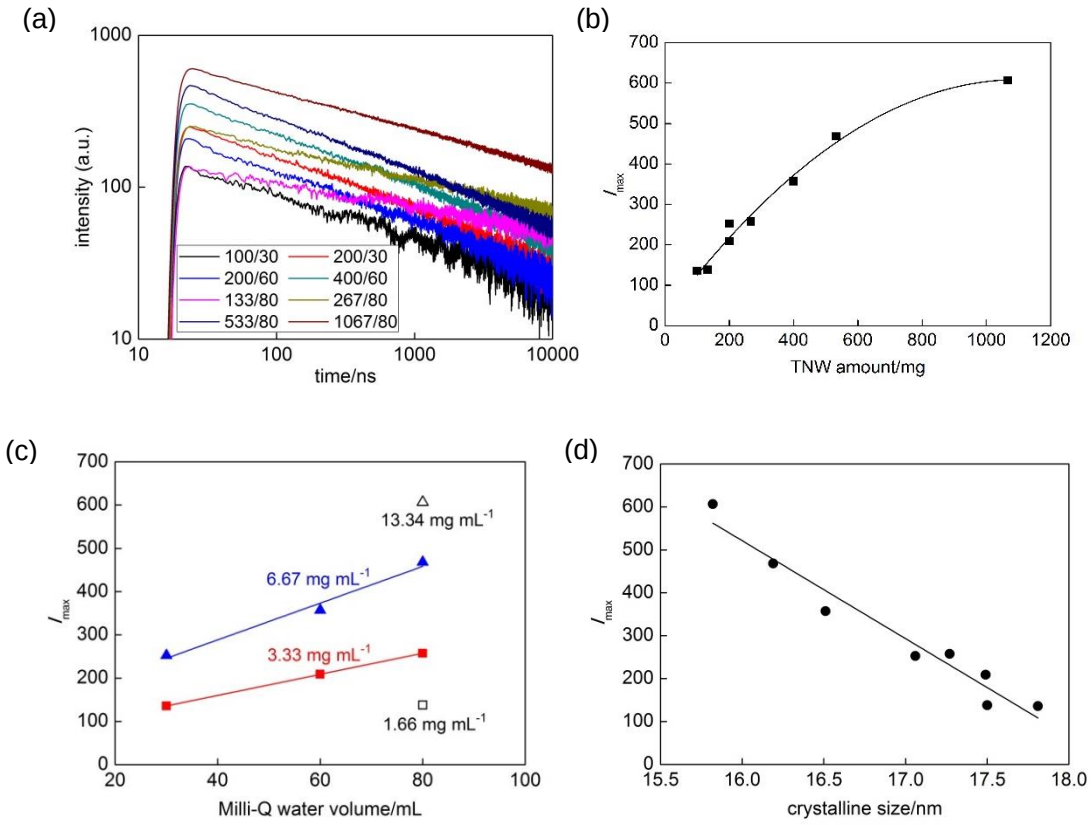

Fig. 4. (a) Time course of TRMC signal, (b) influence of the amount of TNWs on I_{max}, (c) influence of water volume on I_{max}, and d) dependence of I_{max} on crystalline size.

3.1.2. Photocatalytic activity

Our previous study using OAP samples prepared with a constant amount of reagents and different conditions of HT (HT duration, HT temperature and sonication duration) showed that larger OAP content led to higher photocatalytic activity. Data obtained by TRMC and photoacoustic spectroscopy indicated a favorable distribution of shallow ETs on OAP-shaped titania nanoparticles (NPs).

In the present study, all of the samples were prepared with the same conditions of the HT process, and the results obtained for photocatalytic activity are shown in Fig. 5a. For comparison, previous data for samples prepared under the same HT conditions and having almost the same surface properties with the exception of morphology are shown. There was an almost linear correlation between morphology and photocatalytic activity for acetic acid decomposition (CO_2 system) confirming that morphology governs photocatalytic activity. However, the correlation between morphology and photocatalytic activity for methanol dehydrogenation (H_2 system) is not clear and will be discussed further.

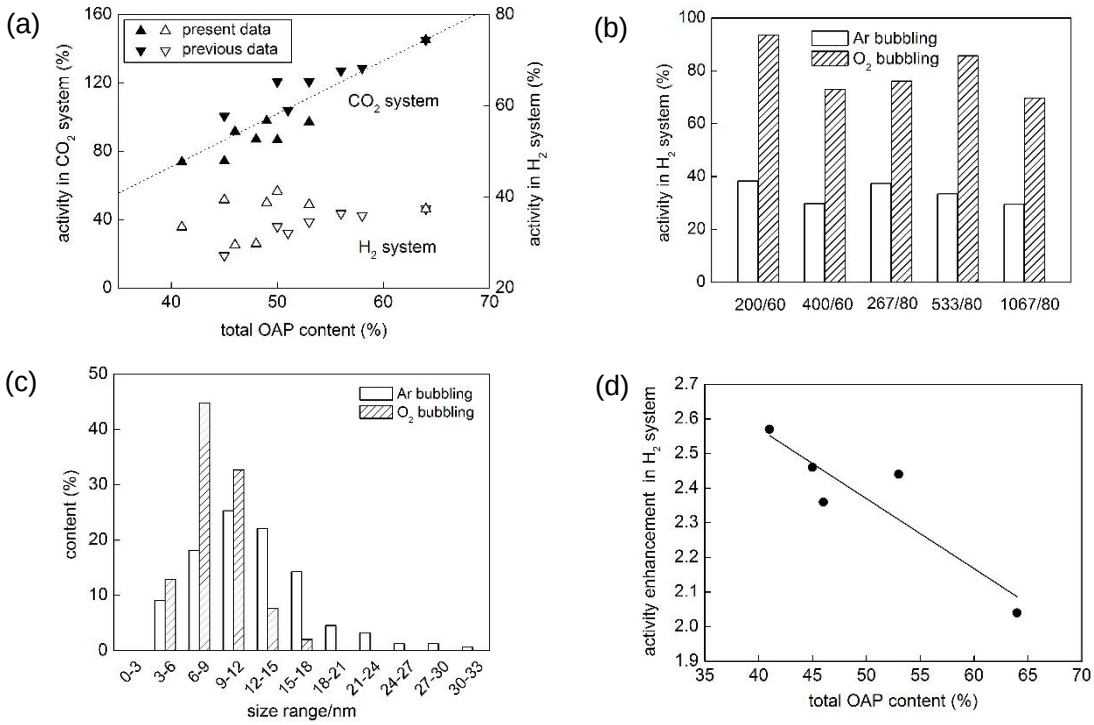

Fig. 5. (a) Influence of morphology on photocatalytic activity: open triangles, H_2 system; solid triangles, CO_2 system, (b) photocatalytic activity in the H_2 system for two kinds of platinum in-situ deposition, (c) platinum particle-size distribution for the 267/80 sample, and (d) dependence of activity enhancement on morphology (from Fig. 5b).

It must be pointed that the content of surface hydroxyl groups can also influence the photocatalytic activity. For example, the 533/80 sample, which had the lowest photocatalytic activity and fastest TRMC signal decay also had the smallest amount of hydroxyl groups on the surface. In contrast, one of the highest contents of surface hydroxyl groups was observed for the 267/80 sample, which had the highest photocatalytic activity. It has been reported that generation of reactive oxygen species depended on surface hydroxylation [19]. Therefore, the content of surface hydroxyl groups might be correlated with density and mobility of electrons. Crystalline defects, e.g., oxygen vacancies are probably responsible for adsorption of hydroxyl groups.

As shown in Fig. 4d, smaller crystalline size resulted in higher intensity of the TRMC signal. Although the signal decays were similar during the first 40 ns, they were noticeably different after 4000 ns (Table S1). The 267/80 and 133/80 samples showed slower decay than that of other samples, but the amount of mobile electrons (I_{max}) in the 267/80 sample was much larger than that in the 133/80 sample. Therefore, the most active sample, 267/80, had relatively high I_{max} and also very slow decay of the TRMC signal. In comparison, our previous results for OAP samples, prepared with the same amount of reagents, showed the same signal decay for all samples, and thus a simple correlation between I_{max} and activity was easily drawn [15]. In the present study, the correlation was more complex, which is typical for titania samples prepared with different synthesis conditions. For example, it was found that I_{max} of the most active titania P25 was one of the lowest among the eight titania photocatalysts, but its signal decay was the slowest [20].

There are a few possible reasons for the low photocatalytic activity of OAPs in the H_2 system. For example, it has been proposed that the presence of two titania facets (001 and 101) is necessary for efficient separation of charge carriers [11]. Indeed, a slight increase in activity with decrease in AR was noticed (Fig. S6), being similar to reported data for rutile nanorods [5, 13] and anatase nanoplates with exposed (101) and (001) crystal facets [21, 22]. It must also be pointed that a co-catalyst (usually platinum deposits) is necessary for this reaction. Therefore, besides properties of titania, the properties of platinum deposits and the interface between titania and platinum are crucial. In the present study, SEM observation indicated that only a small percent of titania particles was in direct contact with platinum, due to the very small sizes of titania particles and aggregation of platinum deposits (Fig. S8, left). Therefore, to slow down the formation of platinum deposits and their aggregation, platinum was deposited in the presence of oxygen ("O_2 pre-bubbling"). Formation of smaller platinum NPs uniformly distributed on OAPs (Fig. 5c and Fig. S8, right) resulted in strong enhancement of photocatalytic activity as shown in Fig. 5b. Interestingly, the enhancement factor was inversely proportional to the morphology (Fig. 5d), indicating that properties of platinum and its contact with titania were more important in the case of samples with worse morphology than that of the 267/80 sample. There is another important function of platinum deposits, i.e., inhibition of charge carrier recombination. Therefore, a lower enhancement factor in the case of titania particles having better morphology indicated a lower rate of recombination of charge carriers (e^-/h^+) in these samples and thus morphology-governed photocatalytic activity. There is another possibility based on results shown in Fig. 5d, i.e., preferential deposition of platinum on non (101) facets in the case of deposition for an oxygen pre-saturated suspension, e.g., on (001) facets, due to blocking of facets by adsorbed oxygen. Therefore, preferential reduction of oxygen on (101) might be the main reason for the high photocatalytic activity of OAPs in the CO_2 system.

3.2. Influence of pH

It is known that pH is one of the most important factors influencing chemical reactions in both heterogeneous and homogeneous systems, and a change of its value may result in the formation of products with greatly different properties such as crystallinity, morphology and thus photocatalytic activity. Therefore, the influence of pH on properties of HT products was investigated for pH values of 3, 6 and 11. HT performed at pH of 6 was named "neutral" since it was the original pH of the reaction suspension without any modifications.

Although phase transition by pH change was reported for HT preparation of anatase from peroxo titanic acid [3], a single anatase phase was obtained in all examined conditions, as shown in Fig. 6. It was found that low pH of the reaction suspension did not influence the crystallinity of the HT product, while basic conditions inhibited HT and only a small amount of TNWs was converted to anatase titania. The sample prepared at pH of 6 showed the highest intensity of the anatase peak. The following chemical equation for the HT process was previously proposed [15]:

$$H_{1.32}K_{0.68}Ti_8O_{17}\cdot 4.0H_2O \rightarrow 8TiO_2 + 4.32H_2O + 0.68KOH$$

Our previous studies showed that pH value of the reaction mixture increased after HT, due to the stoichiometry, from ca. 6 to 12 [9]. The results of the present study indicated that the pH value of the solution influences the conversion of TNWs into anatase titania. It is thought that the TNWs are dissolved and re-crystallized into anatase during the HT process and finally the HT system reaches a dynamic equilibrium between precipitation and dissolution of TNWs, resulting in some wire-like structures remaining in the final product. The conditions of the HT process could influence this dynamic equilibrium. For example, higher temperature and longer duration of HT facilitated the conversion of TNWs into anatase [15]. On the other hand, the basic conditions inhibited this conversion due to the formation of potassium hydroxide.

Acidic conditions did not noticeably influence morphology, and products similar to that obtained in the neutral environment (Fig. 3) were obtained, as shown by SEM observations (Fig. 6). On the other hand, a huge amount of residual TNWs was found in the final product prepared at pH of 11. Elongated nanoparticles were also formed (encircled in Fig. 6), similar to results obtained by Deng et al. suggesting that the presence of OH^- anions changed the surface energy of anatase [23].

The crystalline size did not change noticeably with change in pH (Fig. 7a). The correlation between crystallinity and pH value indicates that the products obtained in acidic and neutral conditions have similar degrees of crystallinity, while the product obtained in the basic condition has very low crystallinity, due to HT inhibition, as was also shown by XRD patterns.

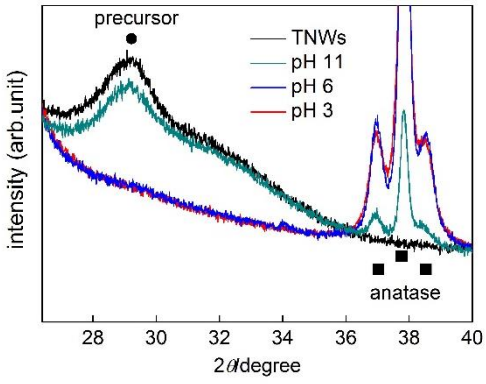

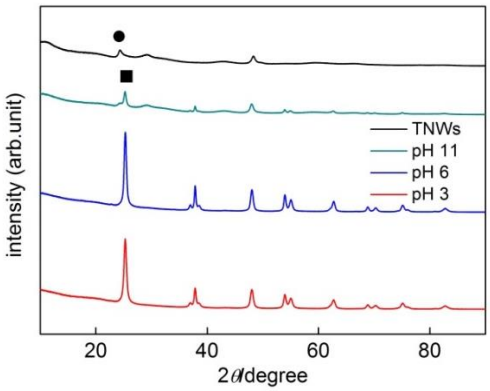

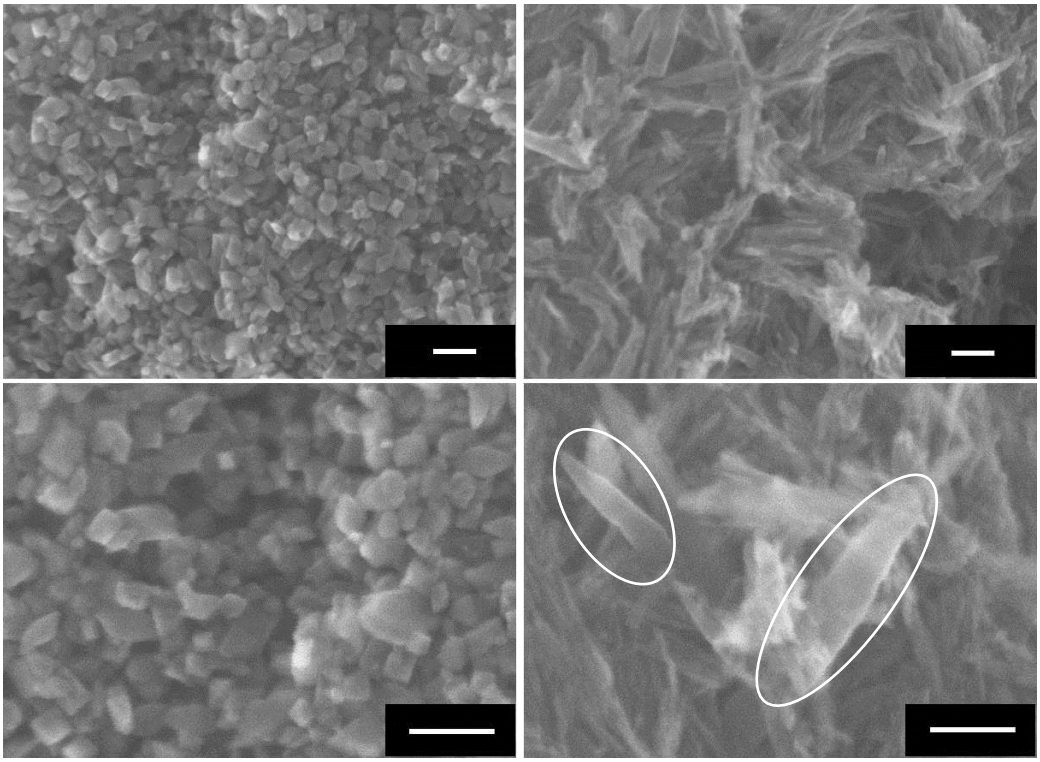

Fig. 6. (top) XRD patterns of TNWs and products obtained at different values of pH, (middle and bottom) SEM images of products prepared at pH values of 3 (left) and 11 (right): Scale bars: 50 nm. Elongated particles are encircled.

It is expected that pH value of the reaction suspension, which influences the morphology, crystallite size and crystallinity of the final products, may also influence the photocatalytic activity. It was found that a higher level of photocatalytic activity was obtained in the neutral condition, especially in the CO_2 system. For dehydrogenation of methanol, acidic and neutral conditions resulted in the same levels of photocatalytic activity, showing the same tendency as pH-dependent crystallinity.

Similar to results for various amounts of reagents (3.1.2), the morphology strongly influenced the photocatalytic activity of the products prepared at different values of pH, as shown in Fig. 7b, especially in the CO_2 system. The photocatalytic activity increased with an increase of total OAP content, showing almost linear dependence.

(a)

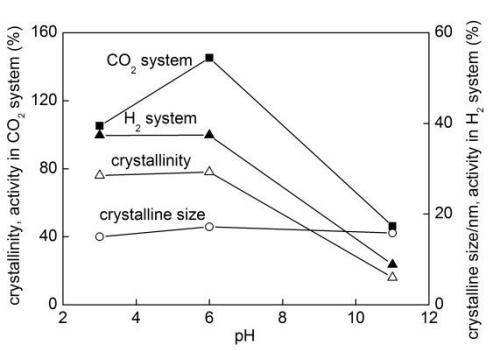

(b)

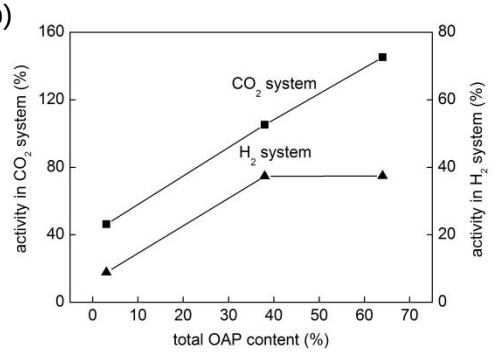

(d)

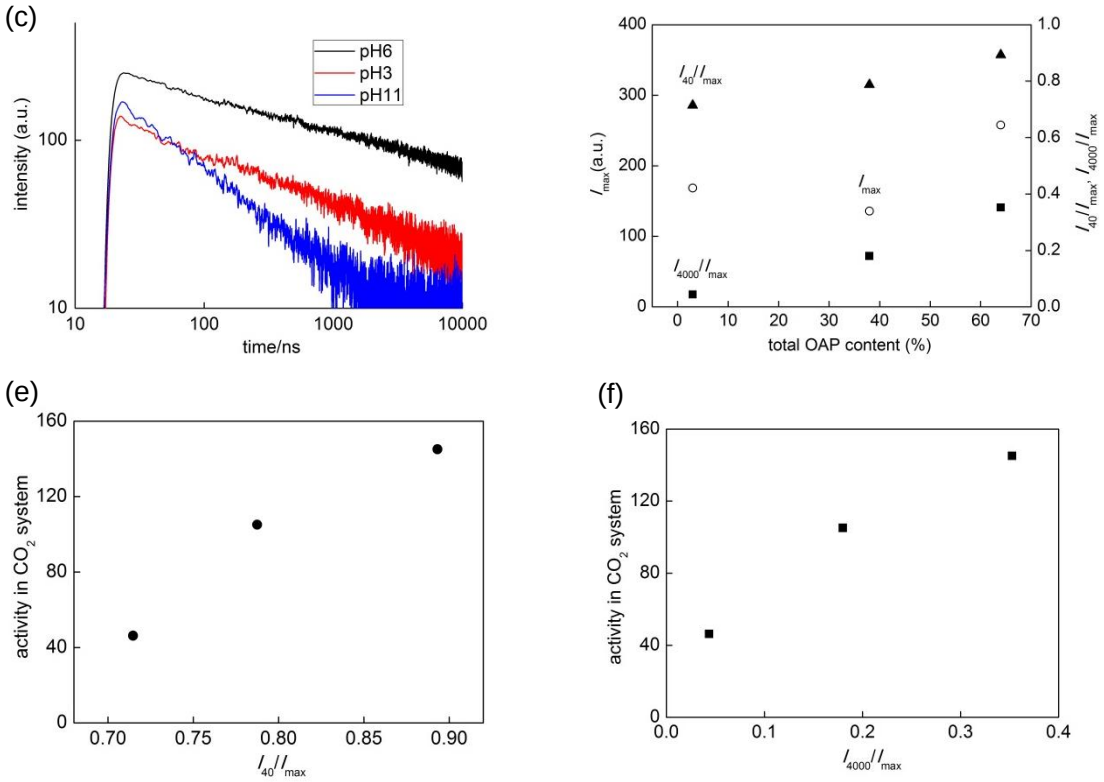

Fig. 7. Influence of pH on properties and photocatalytic activity. (c) Time course of TRMC signals of samples, (d) influence of total OAP content on I_{max}, I_{40}/I_{max} and I_{4000}/I_{max}, (e) influence of I_{40}/I_{max} on activity in the CO_2 system, and (f) influence of I_{4000}/I_{max} on activity in the CO_2 system.

Electronic properties (Fig. 7c and Table S3) showed that pH 6 and pH 3 samples have the highest and lowest I_{max}, respectively. The fastest signal decay, but not the lowest I_{max}, was obtained for the less active pH 11 sample. This confirms that for samples prepared under differed conditions of the HT process, signal decay is a more reliable factor than the value of I_{max} for correlation with photocatalytic activity, suggesting that signal decay directly correlates with the recombination between electrons and holes. Therefore, faster decay means a larger amount of recombination centers, i.e., deep ETs, resulting in lower photocatalytic activity. The influence of morphology (total OAP content) on I_{max}, I_{40}/I_{max}, I_{4000}/I_{max} is shown in Fig. 7d. Although the influence of morphology on the I_{max} value is not clear, the OAP content governs the signal decays, since clear correlations between signal decays and photocatalytic activities were obtained (Fig. 7e-f), confirming that larger OAP content results in a smaller amount of recombination centers and thus in higher photocatalytic activity. These results correspond to the results of our previous study showing that (101) facets are responsible for the preferential distribution of shallow ETs rather than deep ETs. However, a direct correlation between photocatalytic activity and I_{max} value was obtained in our previous study since all of the samples had the same TRMC decay. In the present study, TRMC decay was shown to be a more reliable factor for photocatalytic activity correlation.

4. Conclusions

The properties of titania containing OAPs depend on conditions during the HT process, i.e., pH value, amount of TNWs and water volume. It was found that a higher concentration of TNWs induces deformation of the octahedral shape, due to either a steric effect or squeezing forces. On the other hand, the water volume, and therefore pressure inside the reactor, is crucial for preparation of perfectly shaped crystals at a lower concentration of TNWs. Photocatalytic activity was correlated with decay of the TRMC signal but not with its intensity. This indicates that not the amount of mobile electrons but their detrapping ability, and thus ratio of shallow to deep electron traps in the titania structure governs photocatalytic activity.

The significant influence of the properties of platinum NPs (size and distribution) on photocatalytic activity indicates preferential deposition of platinum on non (101) facets (in the presence of pre-sparged oxygen) and simultaneous reduction of oxygen on the (101) facet. Therefore, it is proposed that this preferential reduction of oxygen on the (101) facet is responsible for high photocatalytic activity of OAPs for oxidative decomposition of organic compounds.

The advantage of OAP morphology exhibiting hindered recombination of electrons and holes was confirmed by TRMC study. Preparation of pure OAP samples (100%) with greatly enhanced photocatalytic activity is the next target. It is thought that an HT process involving several steps (to disturb the dynamic equilibrium of HT) will result in preparation of purer OAP products.

Acknowledgement

This research was funded by the CONCERT-Japan Joint Call.

References

[1] M.R. Hoffmann, S.T. Martin, W.Y. Choi, D.W. Bahnemann, Chem. Rev. 95 (1995) 69-96.

[2] S. Malato, J. Blanco, J. Caceres, A.R. Fernandez-Alba, A. Aguera, A. Rodriguez, Catal. Today 76 (2002) 209-220.

[3] N. Murakami, Y. Kurihara, T. Tsubota, T. Ohno, J. Phys. Chem. C 113 (2009) 3062-3069.

[4] O.O. Prieto-Mahaney, N. Murakami, R. Abe, B. Ohtani, Chem. Lett. 38 (2009) 238-239.

[5] N. Murakami, S. Katayama, M. Nakamura, T. Tsubota, T. Ohno, J. Phys. Chem. C 115 (2011) 419-424.

[6] J.W. Shiu, C.M. Lan, Y.C. Chang, H.P. Wu, W.K. Huang, E.W.G. Diau, ACS Nano 6 (2012) 10862-10873.

[7] F. Amano, T. Yasumoto, O.O. Prieto-Mahaney, S. Uchida, T. Shibayama, B. Ohtani, Chem. Commun. (2009) 2311-2313.

[8] K. Kanie, T. Sugimoto, Chem. Commun. (2004) 1584-1585.

[9] Z.S. Wei, E. Kowalska, B. Ohtani, Chem. Lett. 43 (2014) 346-348.

[10] Z.S. Wei, Y. Liu, H. Wang, Z.W. Mei, J.W. Ye, X.G. Wen, L. Gu, Y.T. Xie, J. Nanosci. Nanotechno. 12 (2012) 316-323.

[11] M. Janczarek, E. Kowalska, B. Ohtani, Chem. Eng. J. 289 (2016) 502-512.

[12] J. Georgieva, S. Sotiropoulos, S. Armyanov, N. Philippidis, I. Poulios, J. Appl. Electrochem. 41 (2011) 173-181.

[13] E. Bae, N. Murakami, T. Ohno, J. Mol. Catal. a-Chem. 300 (2009) 72-79.
[14] C.H. Wang, X.T. Zhang, Y.L. Zhang, Y. Jia, B. Yuan, J.K. Yang, P.P. Sun, Y.C. Liu, Nanoscale 4 (2012) 5023-5030.
[15] Z. Wei, E. Kowalska, J. Verrett, C. Colbeau-Justin, H. Remita, B. Ohtani, Nanoscale 7 (2015) 12392-12404.
[16] Z. Wei, E. Kowalska, B. Ohtani, Molecules 19 (2014) 19573-19587.
[17] S. Uchida, J. Sanehira, J. Patent, P2005-162584A (2005).
[18] N. Murakami, O.O.P. Mahaney, T. Torimoto, B. Ohtani, Chem Phys Lett 426 (2006) 204-208.
[19] S.H. Szczepankiewicz, A.J. Colussi, M.R. Hoffmann, J. Phys. Chem. B 104 (2000) 9842-9850.
[20] Y.V. Kolen'ko, B.R. Churagulov, M. Kunst, L. Mazerolles, C. Colbeau-Justin, Appl. Catal. B-Environ. 54 (2004) 51-58.
[21] M.V. Sofianou, V. Psycharis, N. Boukos, T. Vaimakis, J.G. Yu, R. Dillert, D. Bahnemann, C. Trapalis, Appl. Catal. B-Environ. 142 (2013) 761-768.
[22] M.V. Sofianou, N. Boukos, T. Vairnakis, C. Trapalis, Appl. Catal. B-Environ. 158 (2014) 91-95.
[23] Q.X. Deng, M.D. Wei, X.K. Ding, L.L. Jiang, K.W. Wei, H.S. Zhou, J. Cryst. Growth 312 (2010) 213-219.